

Frederike Alwes · Gerhard Scholtz

Stages and other aspects of the embryology of the parthenogenetic Marmorkrebs (Decapoda, Reptantia, Astacida)

Received: 11 July 2005 / Accepted: 26 October 2005 / Published online: 3 January 2006
© Springer-Verlag 2006

Abstract The early development of the parthenogenetic Marmorkrebs (marbled crayfish) is described with respect to external morphology, cell lineage, and segment formation. Due to its parthenogenetic reproduction mode, the question arises whether or not the marbled crayfish is a suitable model organism for developmental approaches. To address this question, we describe several aspects of the embryonic development until hatching. We establish ten stages based on characteristic external changes in the living eggs such as blastoderm formation, gastrulation process, formation and differentiation of the naupliar and post-naupliar segments, limb bud differentiation, and eye differentiation. The study of the post-naupliar cell division patterns, segment formation, and *engrailed* expression reveals distinct similarities to that of other freshwater crayfish. On this basis, we evaluate the possibility of a generalization of ontogenetic processes in the Marmorkrebs for either freshwater crayfish or other crustacean developmental systems.

Keywords Marbled crayfish · Segmentation · Cell lineage · Engrailed · Astacida

Introduction

Ever since embryologists directed their interest towards the highly diverse group of Crustacea, starting with the classical period of crustacean embryology in the 19th century, freshwater crayfish have been a popular subject of developmental studies (e.g. Rathke 1829; Lereboullet 1862; Huxley 1880; Reichenbach 1888; Fulinski 1908;

Zehnder 1934; Fioroni 1969; Patel et al. 1989a; Scholtz 1992, 1993; Abzhanov and Kaufman 2000a).

Some of the work on crayfish embryology is concerned about the discrimination of different phases during development from the spawned egg until hatching. Based on external morphological characters, the number of characterized stages ranges from five (Rathke 1829) to 11 (Reichenbach 1888) or as many as 15 developmental stages (Zehnder 1934). Sandeman and Sandeman (1991) created a crayfish staging based on steps of 5% of the total developmental time with the hatching embryo as 100%, combined with external morphological characters that are observable in the living eggs. They proposed that their staging scheme of the Australian species *Cherax destructor* is applicable to freshwater crayfish in general (Sandeman and Sandeman 1991). The goal was to provide a scheme of stages as a useful basis for further investigations. This lead was followed by García-Guerrero et al. (2003). Going into more detail, Scholtz (1992, 1995a) traced the cell lineage of the ectoderm and the segment formation of the germ band of *C. destructor*. This study was part of a comparative approach within the Malacostraca addressing developmental and phylogenetic questions (Scholtz 1993; Scholtz and Dohle 1996; Scholtz 1997).

Recently, the Marmorkrebs (marbled crayfish) has gained great interest in being the first described parthenogenetic decapod (Scholtz et al. 2003; Vogt and Tolley 2004; Vogt et al. 2004; Seitz et al. 2005). The question arises as to whether or not this parthenogenetic form shows some peculiarities due to its derived mode of reproduction. This is not a far-fetched assumption as demonstrated by other crustaceans. For instance, the raptorial cladoceran *Leptodora kindtii* shows a direct development in its parthenogenetic phase (Gerberding 1997; Olesen et al. 2003) whereas the bisexually produced embryos hatch as a specialized nauplius larva (Sars 1873).

The first study on the morphology of the principal life stages with emphasis on the post-embryonic development has been done by Vogt and Tolley (2004). Seitz et al. (2005) investigated development, growth, and egg production under different laboratory conditions and proposed the

Communicated by S. Roth

F. Alwes · G. Scholtz (✉)
Institut für Biologie/Vergleichende Zoologie,
Humboldt-Universität zu Berlin,
Philippstr. 13,
10115 Berlin, Germany
e-mail: gerhard.scholtz@rz.hu-berlin.de
Tel.: +49-30-20936005
Fax: +49-30-20936002

first staging system of marbled crayfish development. These studies will now be complemented with the present detailed study on the embryonic development of the Marmorcrebs until hatching. We document our observations on the development of the marbled crayfish in living eggs. Furthermore, we describe morphogenesis in more detail with emphasis on limb development, segment formation, and cell division patterns of the ectoderm using fluorescent dye, immunohistochemistry, CLSM and scanning electron microscope (SEM).

In the discussion, we compare the staging system of Sandeman and Sandeman (1991) and our observations of the marbled crayfish. The staging system in percentages is already commonly used for crayfish (e.g. Scholtz 1992; Abzhanov and Kaufman 2000a,b; García-Guerrero et al. 2003), as well as for other arthropods (e.g. Bentley et al. 1979; Helluy and Beltz 1991; Browne et al. 2005). So far, it is suggested that it is a promising tool for comparisons of different organisms at similar stages. Therefore, we bring the development of the Marmorcrebs into line with the staging of Sandeman and Sandeman (1991), but we also discuss the implications of the percentage method critically. In addition, we refer to some aspects concerning the knowledge about crayfish in general with respect to segment formation, differentiation of ecto- and mesoteloblasts, differential cleavages and morphogenesis of the developing limbs and compare them with our results in the Marmorcrebs.

Materials and methods

Specimens of the Marmorcrebs from a laboratory population established at the Humboldt University of Berlin were kept in a 60 l aquaria either as single individuals at 18°C ($\pm 2^\circ\text{C}$) (seven specimens) or at room temperature at 22°C ($\pm 5^\circ\text{C}$) with up to three adults in a tank (12 specimens). Gravid animals were kept isolated in a 15 l aquaria during brood care.

Living eggs

Freshly laid eggs were taken from the pleon of the mother with tweezers and put into petri dishes filled with tap water. The eggs were immediately observed under a dissecting microscope and documented. For further processing, some eggs were fixed as described below and others were kept in tap water for further development at either 4°C or room temperature. In addition, the remaining attached eggs were taken from the mother's pleon every 24 h and were also observed, documented, and immediately fixed for further processing.

Fixation

Due to the tough egg envelopes, difficulties occurred with respect to the penetration of the fixative. Depending on

stage and consistency, different treatments were required beforehand to ensure a quick penetration of the fixative on the one hand and, on the other, to minimize artifacts during the fixation process: The earliest stages were put into absolute methanol at -8°C for 30 min. This guaranteed that the yolk structure and the cell material were preserved within the envelopes despite the high pressure within the egg. Before that, it is not possible to remove the egg envelopes.

For the SEM procedure the eggs were gently transferred into Bouin's fixation (75% saturated aqueous picric acid solution, 20% saturated formaldehyde, and 5% glacial acetic acid). Egg envelopes were removed manually in Bouin's fixation with dissection needles and tweezers. For fluorescent nuclei staining, eggs were washed in methanol and stored in methanol at -8°C until further processing.

In later stages, in which cell cohesion prevents the collapse of cell structure, the germ was removed manually from the egg shells and the yolk in tap water. It was then immediately transferred into the respective fixative. For nuclei staining or whole mount antibody staining, later stages were fixed for 30–35 min in 3.7% formaldehyde in 1× PBS (1.86 mM NaH_2PO_4 , 8.41 mM Na_2HPO_4 , 175 mM NaCl, pH 7.4). The eggs were also stored at -8°C in absolute methanol for further processing. For the SEM procedure, the dissected eggs were transferred into Bouin's fixation for at least 2 h. The caudal papilla or appendages were immediately folded back or arranged in another way before the embryonic tissue hardened.

Nuclear staining

For staining with the DNA-selective fluorescent dye Hoechst (Bisbenzimidazole, H33258), the preserved and dissected eggs were washed in 1× PBS several times (three times for 5 min and four times for 30 min) and then transferred into Hoechst solution (1× PBS, 0.09% Bisbenzimidazole). Unbound dye was removed by washing in 1× PBS for at least 2 times for 10 min. After embedding in DABCO–glycerol (2.5 mg/ml DABCO (1.4 diazobicyclo-[2.2.2]-octane, Merck) in 90% glycerol–PBS), the eggs were either observed by a fluorescence microscope (Zeiss Axiophot 1) (excitation 352 nm, emission 461 nm) or by a laser scanning microscope (Leica SP2). Digital images emerged from a Nikon D1 digital camera were partly adjusted in brightness and contrast using Photoshop 6.0 (Adobe). Picture piles emerged by the confocal laser scanning microscope were processed and edited with the 3-D reconstruction software IMARIS (Bitplane AG, Zürich).

Whole-mount antibody stainings

Antibody staining was performed essentially by using standard protocols (Patel et al. 1989b). The washing procedure was done in PBT (1× PBS, 0.2% BSA, 0.1% Triton x-100). Incubation in the *engrailed* antibody Mab 4D9 (mouse IgG1 monoclonal) solution was done in

200- μ l antibody solution (supernatant and PBT+N [PBT, 5% NGS (normal goat serum)] in same volumes) at 4°C overnight. As secondary antibodies, we used either alkaline-phosphatase-conjugated goat-anti-mouse IgG (Jackson Immunoresearch) or peroxidase-conjugated goat-anti-mouse IgG (Jackson Immunoresearch) (each 1:200 in PBT+N) again at 4°C overnight. The developing procedure followed standard protocols for each conjugated enzyme. The embryos were counterstained with the fluorescent dye Hoechst (Bisbenzimidazole, H33258) and mounted in DABCO-glycerol as described above.

Scanning electron microscope (SEM)

The Bouin's fixed and dissected embryos were dehydrated gently in an increasing ethanol series (5% steps up to absolute ethanol). The embryos were critical-point-dried by a CPD BALTEC 030 with CO₂ as transitional fluid. The mounted specimens were sputter-coated with gold using a SCD BALTEC 005. Scanning electron microscopy was done with a Leo 1450VP (Leica) and documented by digital photographs. Digital images were edited using Photoshop 6.0 (Adobe).

Results

Like freshwater crayfish in general, the Marmorkebs develops directly, hatching as a non-feeding individual at the first post-embryonic stage (Scholtz 2002). This stage is then followed by a second non-feeding post-embryonic stage before the juvenile reaches the habitus of the adult (Vogt and Tolley 2004). Thus, the complete set of segments and tagmata is differentiated before hatching. First, the naupliar segments of the so-called egg nauplius are formed nearly simultaneously, leading to the prospective first and second antennal and the mandibular segments. Subsequently, the first two post-naupliar segments, the first and second maxillary segments, are formed. The following post-naupliar segments, leading to the eight thoracomeres and to the six pleomeres, are generated by the ectoteloblastic growth zone which proliferates cell material in the anterior direction. Beyond the sixth thoracic segment, the subsequently proliferated segments are formed ventrally as well as dorsally by the ectoteloblast ring enclosing the caudal papilla anterior to the telson. The naupliar appendages, namely the first and second antennae, and the mandibles appear first, followed by the first and second maxillae. The limb buds of the first three thoracic appendages specialized as maxillipeds develop more or less at the same time as incipient ventral protuberances. The fourth to eighth thoracomeres bear the uniramous walking legs to which we refer as the five pereopods. The pleon is composed of six pleonic segments of which, in the hatchling, the second to fifth pleonic segments each bear a pair of biramous pleopods. The sixth segment bears the anlagen of the uropods which later form the tail fan together with the telson (Vogt and Tolley 2004; Vogt et al. 2004).

Characterization of ten developmental stages in the embryonic development

In the following characterization, the externally visible observations on the marbled crayfish is aligned with the percentage staging of *C. destructor* by Sandeman and Sandeman (1991). However, the duration of the entire development until hatching varies depending on the age of the mother and other environmental circumstances such as temperature (see Seitz et al. 2005). Moreover, even within one clutch the eggs show considerable differences in their developmental level, despite homogeneous temperature conditions (see also Seitz et al. 2005). Therefore, we find it reasonable to discriminate ten stages for practical use by conspicuous external features characterizing development in rough outlines which will mainly refer to the 10% steps in Sandeman and Sandeman (1991) and Seitz et al. (2005). The description of the stages will be endorsed by going into more detail in fixed and stained embryos.

Stage 1: the first cleavages and the formation of the blastoderm

The marbled crayfish is characterized by having relatively large and yolky eggs that undergo a superficial cleavage. The egg membrane itself is enclosed by a strong envelope composed of an embryonic endochorion and a maternal exochorion as described for *Astacus fluviatilis* and *Astacus torrentium* (now *Astacus astacus* and *Austropotamobius torrentium*) by Zehnder (1934). The egg has a strictly spherical shape of about 1,300 to 1,500 μ m in diameter. The color of the yolk varies between dark brown and yellowish brown (Fig. 1).

The first mitotic events take place in the center of the egg without external expression (Fig. 1a). First appearance of the nuclei as whitish spots occurs at a number of about 128 nuclei. During the next mitotic waves, the nuclei reach the egg surface. The cell membranes start to groove into the yolk mass and outer cell segmentation becomes visible. The structure of the yolk within these cells becomes more granular. Finally, due to the synchronous mitotic process in all nuclei, a regular blastoderm is formed in which each cell is surrounded by six neighbor cells (see Fig. 2a). Note the ratio of the cell volume and the nuclei size in Fig. 2b at the blastoderm stage compared to that in later stages, e.g. in Fig. 2f.

Stage 2: the formation of the germ disc and the beginning of gastrulation

The formation of the germ disc can hardly be observed in the living eggs. It can be localized as soon as the blastopore has formed as a horseshoe-like furrow with the opening to the posterior. This furrow deepens more and more until it forms an orbital furrow of about 350 μ m in diameter

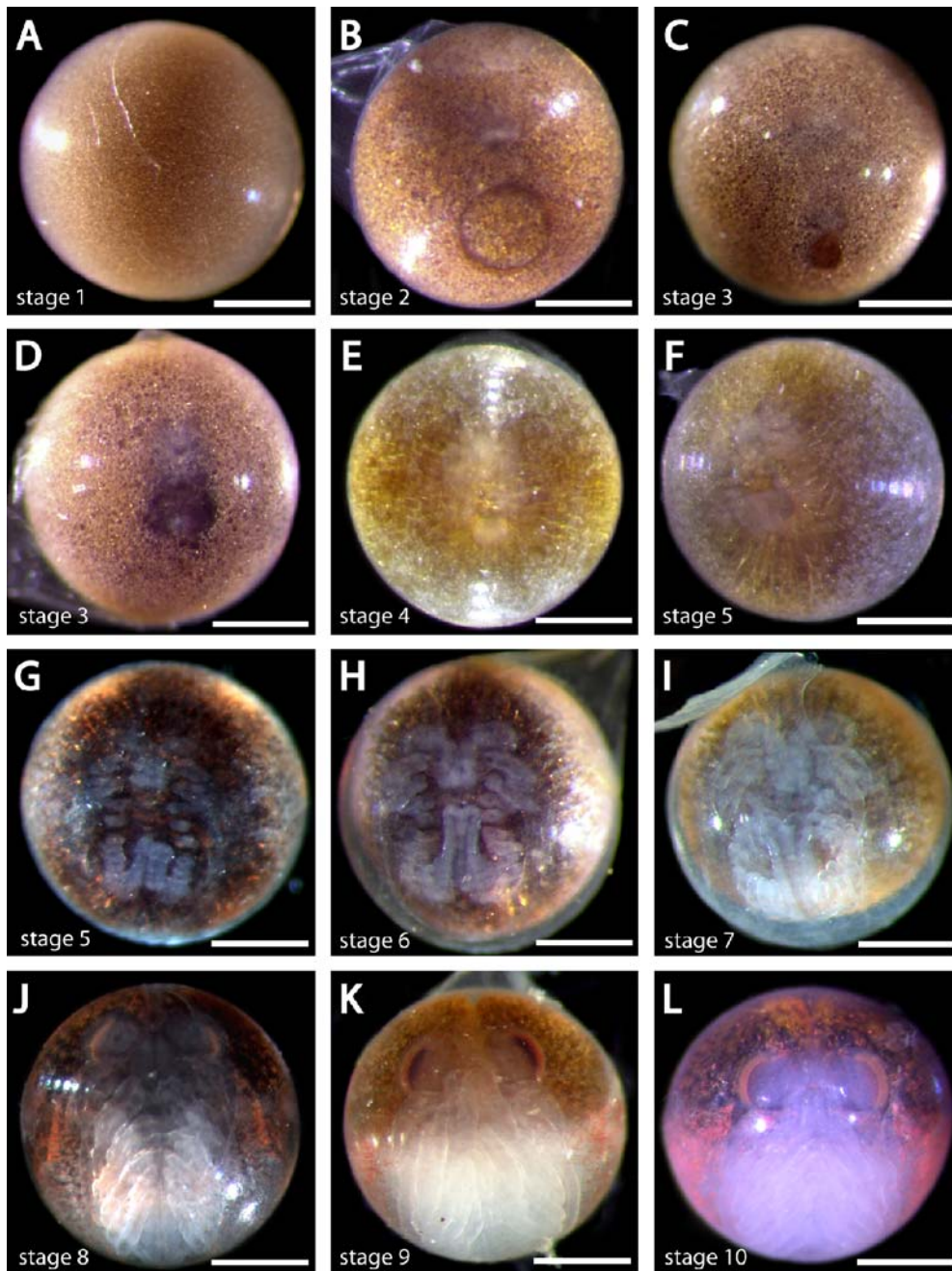


Fig. 1 Developmental stages of unfixed embryos exemplifying the ten characteristic stages. Scale bar=500 μm . **a** Stage 1: the egg without external signs of the cleavage process. **b** Stage 2: the beginning of gastrulation results in the formation of a circular blastopore of about 300 μm in diameter. **c** Stage 3: the caudal papilla adjacent to the closing blastopore and the two optical lobes are visible as *whitish regions*. The closing blastopore appears as a contracting *dark patch* posterior to the germ disc. **d** Embryo at the end of stage 3: the recruitment of cell material of the naupliar anlagen is advanced and the blastopore is now closed. Beneath the posterior half of the germ, the restructuring yolk appears as a *dark diffuse cloud*. **e** Embryo at the end of stage 4: the dark patch has disappeared and the yolk is reorganized. The caudal papilla is bent

ventrally from now on. **f** Stage 5: the caudal papilla is flexed and its tip reaches the margin of the second maxillary buds. **g** Embryo at the beginning of stage 6. The tip of the caudal papilla reaches the segment of the second maxillae. **h** Stage 6: the tip of the caudal papilla now reaches the posterior margin of the mandibles. **i** Stage 7: the thoracopods are arranged like a basket. **j** Stage 8: the pereopods cover the caudal papilla, but do not meet at its midline. The retinal pigmentation begins as *yellowish stripes* below the outer eye margin. The *orange* chromatophores of the carapace appear. **k** Stage 9: the tips of the chelae of the first pereopods nearly overlap the rostrum between the eyes. The advanced retinal pigmentation has turned the yellowish stripes into distinct *brown* retinal layers. **l** Stage 10: the prehatchling

surrounding the transparent mesendodermal tissue (Fig. 1b). Adjacent to the blastopore, the early caudal papilla anlage appears as a white cell cluster (Fig. 1b). Anterior to the

caudal papilla anlage, the initial V-shaped germ disc forms by the incipient accumulation of the cell cluster of the optical lobes (Fig. 2c). Nuclei stainings of fixed embryos

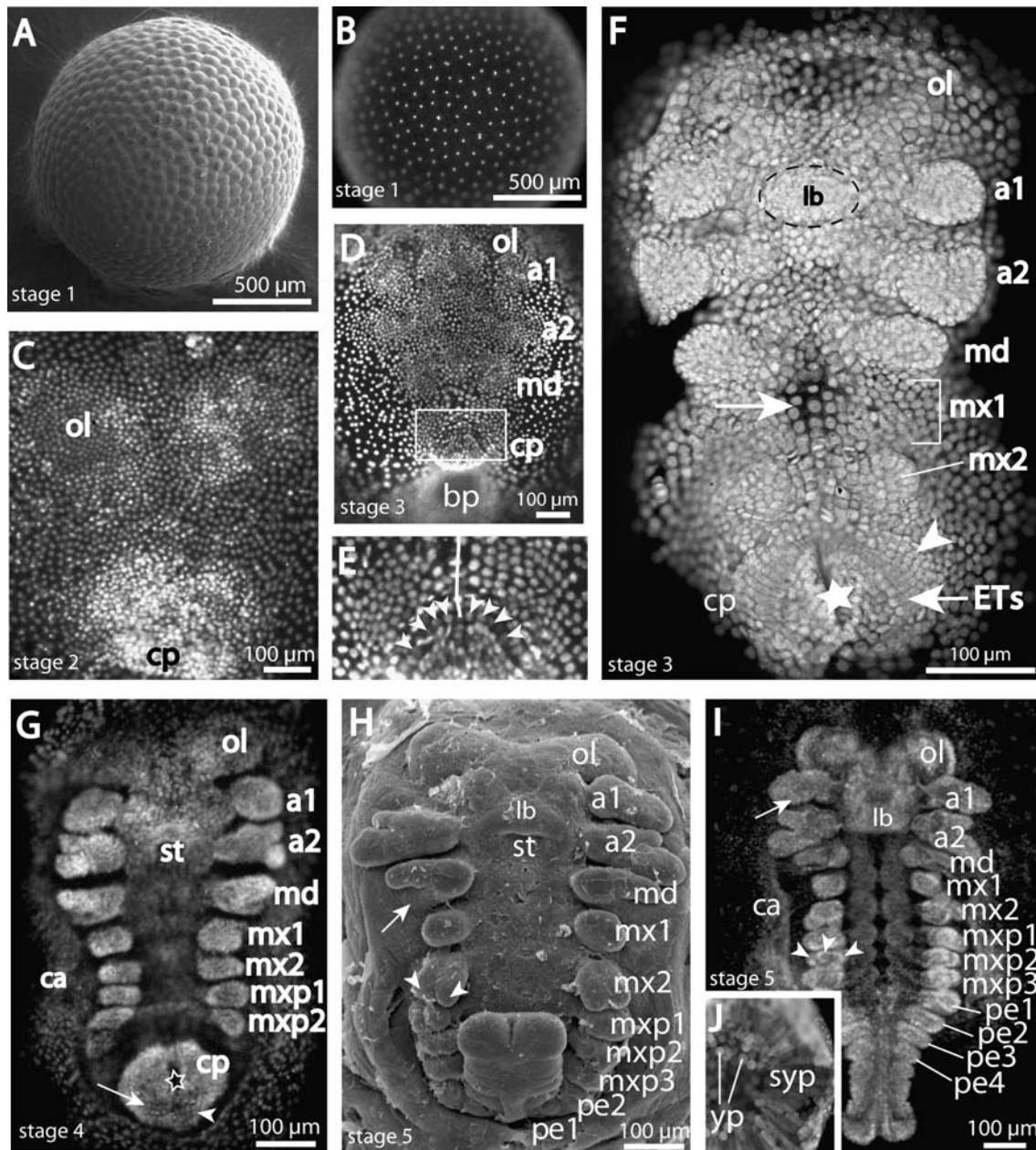


Fig. 2 **a** SEM of the blastoderm stage in which the blastoderm cells uniformly cover the egg surface at the end of stage 1. **b** Blastoderm at the same developmental stage as in **(a)** stained with the fluorescent nuclei dye Hoechst. The nuclei appear as *small spots* within the comparatively large blastoderm cells. **c** Early *V-shaped* naupliar Anlagen without regular cell division pattern at stage 2 (Hoechst staining). First cell groups that become dense anterior to the caudal papilla (*cp*) are distinguishable as the optical lobes (*ol*). **d** Early formation of the naupliar segments during stage 3 (Hoechst staining). The blastopore (*bp*) is still open. First antennae—*a1*, second antennae—*a2*, caudal papilla—*cp*, mandibles—*md*, optical lobes—*ol*. **e** Detail of the growth zone anterior to the caudal papilla [white rectangle in **(d)**]. White arrowheads point to the first differentiated ectoteloblasts around the ventral midline (white line). **f** Beginning of the formation of the post-naupliar segments at the end of stage 3 (Hoechst staining). Protrusions of the naupliar segments have enlarged to defined buds (*a1*, *a2*, and *md*). No formation of buds in the segment of the first maxillae (*mx1*) can be detected at this stage, whereas the second maxillae (*mx2*) already appear as defined buds. In the midline region of the *mx1* segment, the cells slightly drift laterally (white arrow). Teloblastic ectoderm (arrowhead) posterior to the segment of the second maxillae (*mx2*)

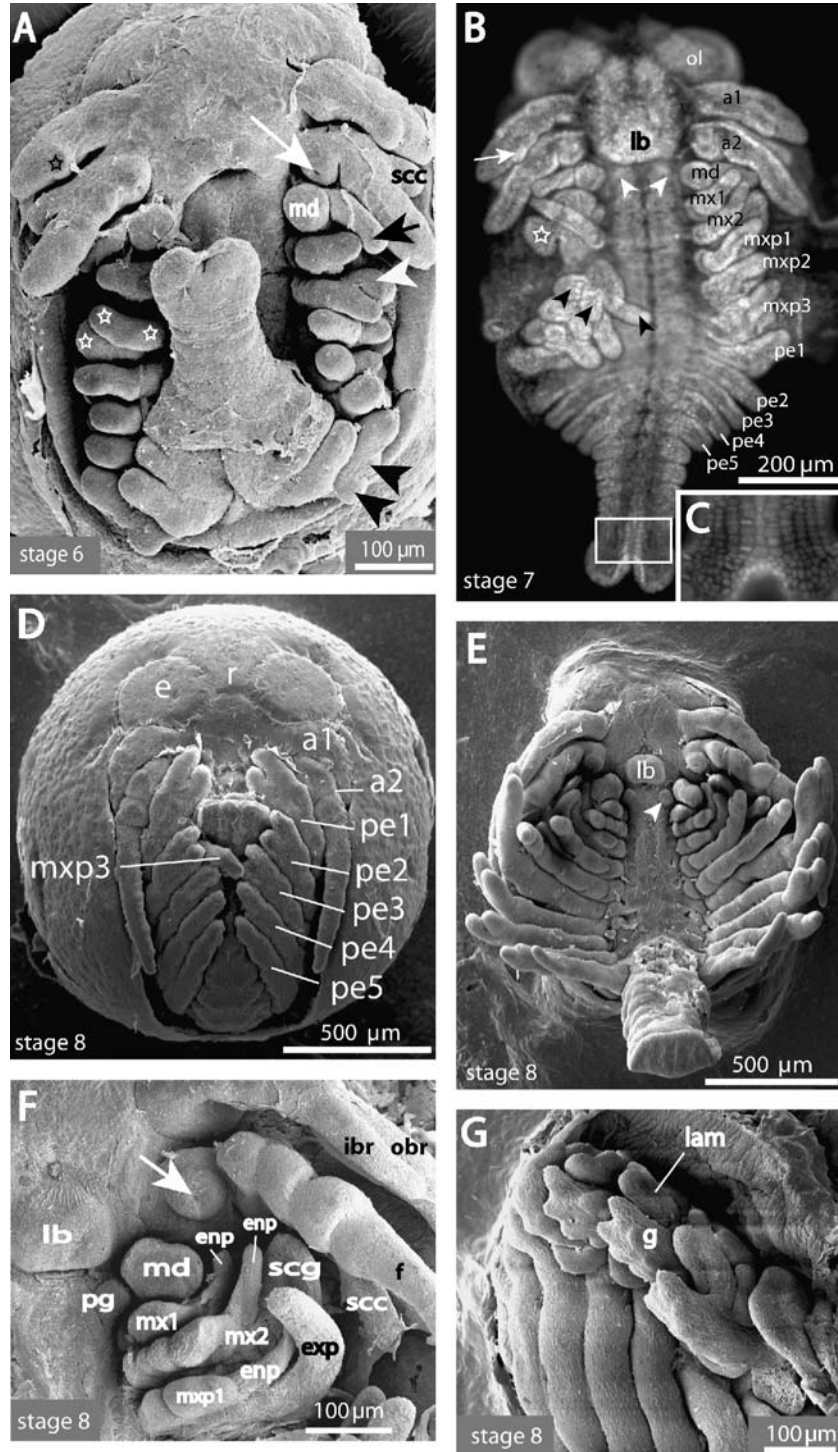
is proliferated by the ectoteloblasts (*ETs*) that are nearly recruited completely (arrowhead) apart from the posterior-most side. The area of the prospective labrum (*lb*) is marked by the broken line. The opening of the proctodaeum is designated by a star. **g** Advanced teloblastic ectoderm formation of an embryo at stage 4. The buds of the first and second maxillipeds (*mxp1* and *mxp2*) are visible as round buds. The formation of the buds of the first maxillae has caught up compared to that of the more posterior buds. **h** Embryo at stage 5 in which the limb buds up to the second pereiopod (*pe1* first pereiopod, *pe2* second pereiopod) appear (SEM). Whereas the first maxillae are still uniramous, the limb buds of the second maxillae, and the first two maxillipeds start to split into endo- and exopodite (designated by arrowheads for the right second maxilla). The arrow points to the basal socket of the mandible. **i** Late stage 5 embryo with the caudal papilla folded back: the limb buds from the second maxillae to the third maxilliped show three protuberances (indicated by white arrowheads here for the *mxp2*). The five pairs of pereiopods appear as lateral projections. The arrow shows the punctiform protrusion of the inner branch of the first antennae. **j** View of the inside of an egg at stage 5. The secondary yolk pyramids (*syp*) have formed except in the immediate center of the egg, where pellet-shaped yolk (*py*) is still left

reveal no regular ectodermal cell division pattern during the formation of the V-shaped germ.

Stage 3: the closing of the blastopore and the formation of the naupliar segment anlagen

This stage is characterized by the closing blastopore which progressively appears as a dark, ovoid patch (Fig. 1c). The

naupliar segment anlagen, the optical lobes, the first and the second antennae, and the mandibles, are already visible, while the blastopore is still open (Fig. 2d). These naupliar segments emanate from the circumjacent blastoderm cells almost simultaneously (Figs. 1c and 2d). During this stage, the formation of the buds of the naupliar appendages results into well-defined protuberances, more or less arranged in a circle (Fig. 2f). Strikingly, the second maxillary buds are visible anterior to the caudal papilla, while the first



maxillary segment reveals no buds at this developmental level (Fig. 2f). Near to the midline of the first maxillary segment, the ectodermal cells slightly drift aside (Fig. 2f).

The first antennae, the mandibles, and the second maxillae appear round-budded and the second antennae broaden distally, indicating the beginning of their characteristic biramous shape (Fig. 2f). In the center, the stomodaeum appears as a small dark cavity in the living egg, but has not invaginated yet (Figs. 1d and 2f). Anterior to the prospective stomodaeum, the cell cluster of the prospective labrum forms (Fig. 2f). The caudal papilla is not yet flexed forward (Figs. 1d and 2f). Its shape is nearly triangular with the tip pointing to the anterior. A median groove ends up posteriorly into the opening of the proctodaeum (Fig. 2f). A dark diffuse region occurs in the living eggs beneath the rear of the embryo (Fig. 1d) caused by the restructuring of the yolk to the so-called secondary yolk pyramids (terminology after Fioroni 1969, 1970; see Fig. 2j of a later embryo). At the end of this stage, the blastopore is closed.

Stage 4: the formation of the first 'post-naupliar segments'

The dark patch caused by the yolk reorganization beneath the embryonic tissue enlarges until it has spread under the entire embryo. The naupliar region has increased in size compared to the rest of the embryo (Fig. 1e). The stomodaeum invaginates and, anterior to the stomodaeum, the

bulge of the labrum is apparent. The second antennae are split distally into two lobes (Fig. 2g). The anterior lobe gives rise to the exopodite and the prospective scaphocerite (the antennal scale), and the posterior lobe gives rise to the three distal basal joints and the annulated antennal flagellum. The mandibles assume a more lateral position, dissolving the circular bud arrangement in the naupliar region. The distal parts of the mandibles slightly project laterally to form the first protrusion of the mandibular palps (Fig. 2g). The first and second maxillae and the first two maxillipeds appear as spheroidal protruberances. The first maxillae have nearly caught up in development to the level of the second maxillae, but they still remain slightly delayed in morphogenesis in the following stages (see below). The caudal papilla is now starting to flex to the anterior, concealing the medioventral parts of the segments of the second and third maxillipeds (Figs. 1e and 2g). Its triangular shape is still apparent, but it is interrupted by the median groove, with the proctodaeum opening dorsally at the tip of the caudal papilla, the telson anlage (Fig. 2g). The carapace anlagen occur as small longitudinal elevations lateral to the germ band starting from the segment of the first maxillae to posterior (Fig. 2g).

Stage 5: the formation of the pereopods

During this stage, the pereiomeres differentiate the limb buds of the pereopods, which more or less protrude laterally from the caudal papilla as round buds. The yolk has become restructured throughout the egg and the secondary yolk pyramids are visible through the nearly transparent embryonic tissue (Figs. 1f and 2j). The limb buds of the second maxillae and the three maxillipeds, and the early buds of the pereopods are visible (Fig. 1f). The buds of the first maxillae are still undivided (Fig. 2h,i). During this stage, the labrum starts to overgrow the stomodaeum. The anterior part of the caudal papilla shows at its lateral sides the incipient segmentation of the more posterior pereiomeres. The opening of the proctodaeum successively moves from the more dorsal side to the tip of the caudal papilla. The caudal papilla is now flexed to the posterior margin of the second maxillary limb buds (Fig. 1g). The carapace anlagen flank the thoracopods, narrowing between the first and second maxillary segments (Figs. 2h and 4b).

The naupliar buds still point laterally and elongate distally. The first antennae show a very small punctiform protrusion in the distal half at the more posterior region (Fig. 2i). This protrusion is the first outgrowth of the prospective inner branch of the first antenna. The second antennal lobes are distinguishable in size: the smaller scaphocerite and the outgrowing projection leading to the basal joints and the antennal flagellum. The latter protrude beyond the mandibular palps. The mandibular palps are discernible from the spherical gnathobasal parts of the mandible (Fig. 2h,i). As shown in Fig. 2h, the gnathobasal part of the mandible is laterally connected with the elevated cell material of the carapace anlage.

◀ **Fig. 3** **a** Embryo at stage 6 (SEM). The bud of the inner branch of the first antennae is designated with the *black star*. The opening of the antennal gland in the most proximal joint of the antennae is apparent (*white arrow*). To the posterior, the antennal scaphocerite (*sc*) is visible as a small bud. *White arrowhead* points to the scaphognathite anlage. Note the protrusions of the first pereopod giving rise to the podobranchial gills (*black arrowheads*). *Stars* mark the three buds of the maxillipeds. **b** Embryo at the beginning of stage 7 with the caudal papilla folded back in which the ectodermal segment formation is nearly finished (Hoechst staining). The first to third maxillipeds of the right body side are folded laterally to have a view on the three-lobed first maxilliped with the external gill anlage, the exopodite in the middle and the endopodite, here pointing to the midline (*black arrowheads*). The *white arrowheads* point to the buds of the paragnaths. The *white arrow* points to the punctiform protrusion of the inner branch of the first antennae. *White star* scaphognathite, *lb* labrum. **c** Detail of the ventral view of the caudal papilla [*white rectangle* in (**b**)] showing the end of teloblastic segment formation. **d** SEM of an embryo at stage 8 in which only the egg membranes are removed, representing the external habit of this stage. *r* rostrum. **e** Ventral view of an embryo at stage 8 with the caudal papilla folded back (SEM). Paragnaths are protruded as clear round buds median to the mandibles (*arrowhead*). **f** Embryo of stage 8 (SEM). Detail of the left side of the appendages involved in feeding (exclusively the second and third maxilliped). The arrow points to the opening of the antennal gland. Endopodite—*enp*, exopodite—*exp*, flagellum of the second antenna—*f*, inner branch of the first antenna—*ibr*, outer branch of the first antenna—*obr*, paragnaths—*pg*, scaphocerite—*sc*. **g** View from anterolateral on an embryo at the same stage as in (**d**) and (**e**). The carapace is removed so that the inner cavity of the respiratory space is visible. Trichobranchiate gill—*g*, branchiate lamella—*lam*

Posterior to the caudal papilla beneath the carapace anlage, the heart is visible in the living eggs as a transparent blister. It pulses very slowly and irregularly. Dorsally, the yolk reveals a slightly darker band-shaped region along the longitudinal axis in the region of the prospective dorsal vessel.

Stage 6: the formation and differentiation of the pleomeres

The caudal papilla is bent ventrally with the tip median to the posterior margin of the mandibles (Figs. 1h and 3a). The proctodaeum opens terminally. The first and second antennae start to direct the distal parts to the posterior (Figs. 1h and 3a). The buds of the inner branch of the first antennae slightly enlarge (Fig. 3a). The second antennae still flank the mandibular palps, with the tips of the antennal flagellae reaching the transversal line of the anterior margin of the first maxillae. At the basal part of the second antennae, the opening of the antennal gland is visible (Fig. 3a). The margins of the carapace anlagen surround the embryonic anlagen conspicuously in the living eggs from the first maxillary segment around the rear (Fig. 1h).

The first differentiation of the post-naupliar limb buds begins in the second maxillae and the three maxillipeds, while the differentiation of the first maxillae is delayed. The second maxillae form two lobes distally, of which the more lateral and enlarged lobe will give rise to the scaphognathite, the ventilation device in the later branchial chamber (Fig. 3a). The first maxillae become biramous when the second maxillae already show basal cleavages leading to the medioproximal endites (Fig. 3a).

The maxillipeds divide distally into three lobes (Fig. 3a): the inner lobe will give rise to the endopodite, the median lobe to the exopodite, and the most lateral to the gill anlagen (epipodites). The limb buds of the pereopods are uniramous during this stage, but first buds occur at the first pereopods, forming the prospective podobranchial gills (Fig. 3a). The subsequent pereopods project laterally from the posterior part of the flexed caudal papilla, gradually elongating from the posterior to the anterior (Fig. 1h).

Observations of the living eggs reveal that the heartbeat is now strong and regular. Dorsally, the yolk broadly grooves longitudinally, indicating the beginning of differentiation of the dorsal vessel.

Stage 7: the elongation of the thoracic limbs (maxillipeds and pereopods)

Both the first and the second antennae point to the posterior more clearly (Fig. 1i). The endo- and exopodites of the maxillipeds are still visible in the living eggs. The differentiation of the first and second maxillae, and of the maxillipeds proceeds by elongation of the endopodites, the differentiation of the exopodites and the 'out-carving' of the gnathal endites from the basal part of the anlagen (Fig. 3b). The tips of the endopodites of the third

maxillipeds enlarge and start to grow over the caudal papilla (Fig. 1i). The five pereopods increasingly elongate and are arranged with the maxillipeds in a basket-like form in the living egg (Fig. 1i). The teloblastic formation of the six pleomeres ends during this stage and the teloblasts no longer exist (Fig. 3c). The opening of the proctodaeum successively moves from the terminal position to a more ventral position within the telson. The carapace anlage broadens to the dorsolateral direction. No pigmentation is apparent during this stage (Fig. 1i).

The paragnaths occur as small round buds in the mandibular segment median to the mandibles. This is only visible in fixed eggs with the appendages and the caudal papilla folded back or removed (Fig. 3b). The paragnaths later form the posterior edge of the mouth region as a functional lower lip.

Stage 8: the differentiation of the pereopods

The caudal papilla elongates and the tip of the caudal papilla reaches the basis of the first antennae. The pereopods now cover the caudal papilla, but do not meet yet in the midline (Fig. 1j). The tips of the endopodites of the third maxillipeds project under either the second or third pereopods (Fig. 3d). The first pereopods are differentiated as large chelipeds (Figs. 1j and 3d). The second and third pereopods also show a first differentiation of chelae (Fig. 3d). The chelae of all three anterior pereopods appear as round-budded branches. The tips of the first antennae are concealed by the second antennae and the margins of the carapace (Fig. 3d). The basal part of the second antennal flagellae has differentiated into three segments (Fig. 3e,f). The tips of the flagellae reach the basal segments of the fourth and fifth pereopods (Fig. 3d). The first and second maxillae have differentiated into the gnathobasal parts, a stalk-shaped endopodite, and the exopodite which in the second maxillae already appears as the characteristically flattened form of the scaphognathite (Fig. 3f). As shown in Fig. 3g, the podobranchial anlagen differentiate in their morphology, giving rise to the trichobranchiate gills and the branchiate lamellae.

First pigmentation of the retinula cells occurs at the anterior margin of the eyes as an incipient yellow stripe (Fig. 1j). Scattered chromatophore dots are distributed over the dorsal margin of the carapace which gradually grows dorsally.

Stage 9: the differentiation of the eyes

The chelipeds more or less reach the tip of the pronounced and elongated rostrum between the eyes (Fig. 1k). They are flanked by the other pereopods, covering the caudal papilla completely (Fig. 1k). The tips of the chelipeds are more pointed now. The eyes are characterized by the pronounced pigmentation in which the pigments of the retinal cells occur as a dense brown stripe (Fig. 1k). The amount of yolk decreases to nearly half of the egg, being increasingly

displaced by the embryonic tissue. It increasingly appears to be curved by the dorsal vessel that successively sinks into the inner of the embryo. The carapace now laterally covers more than half of the embryo (Fig. 1k).

Stage 10: the prehatchling

The amount of yolk now represents the yolk stock remaining at hatching and during the first non-feeding post-embryonic stage. The first pereopods cover the rostrum between the eyes (Fig. 1l). The complete set of segments with the extremities as found in the hatchling are differentiated. The prehatchling appears to be compressed within the egg indicating that the hatching event is imminent.

Conjoined twins

The occurrence of conjoined twins at stage 5 could be detected in a clutch in which the other embryos followed normal development. The individuals are fused at the head, sharing an optic lobe, and one anlage of the first antenna (Fig. 4a). The labrum is separated in both individuals. From the mandible on, each individual consists of a paired set of limb buds as it is expected for this developmental stage. The carapace anlagen at the fused region is shortened and it ends posterior to the margin of the second maxillipeds. The carapace anlagen on the opposite body half of the individuals are elongated and fused so that this anlage surrounds the entire conjoined twins (Fig. 4a).

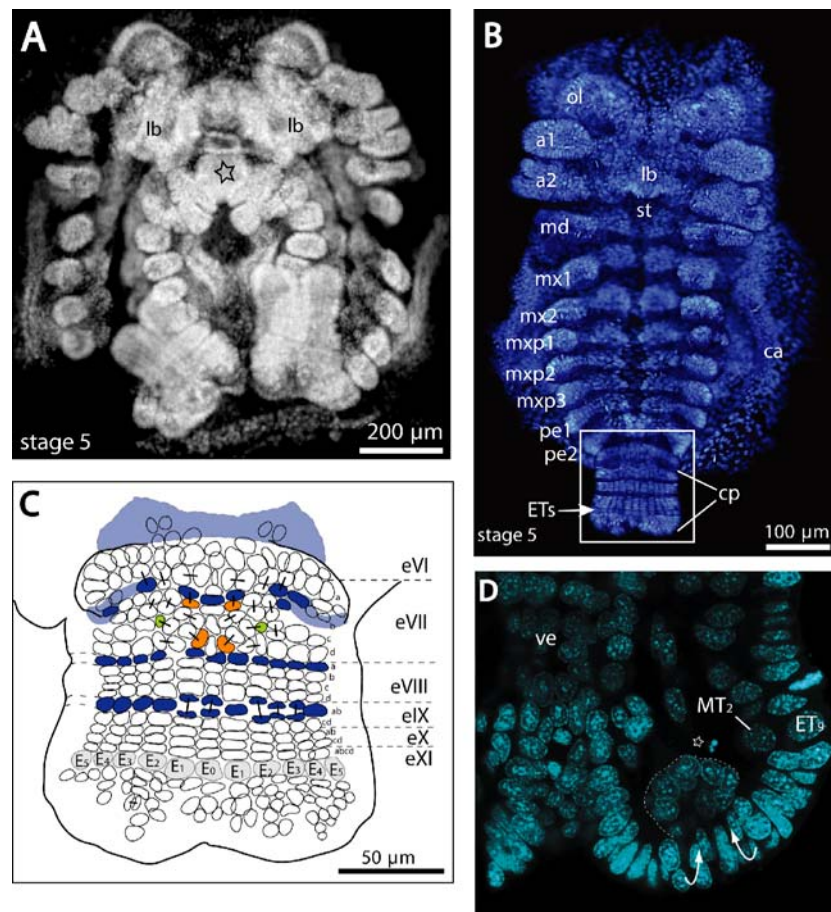


Fig. 4 a These conjoined twins at late stage 5 were found in a clutch in which the other embryos developed normally. They are fused in the head region sharing an optical lobe and one first antenna (*star*), while each of the individuals has a labrum (*lb*). **b** Ventral view of an embryo at stage 5, in which the *engrailed* expression pattern is counterstained with the nuclei fluorescent dye Hoechst (fluorescence quenched). *engrailed* is expressed in the posterior region of each segment. **c** Schematic detail of the ventral view of the caudal papilla during the formation of rows eVI to eXI [projected from the embryo shown in (**b**)]. A ring of about 40 ectoteloblasts (*ETs*) proliferates cell rows to the anterior (here E_0 and E_1 to E_5 on each side are shown). These cell rows each undergo two mediolateral mitotic waves forming a grid-like pattern consisting of the

transversal rows a, b, c, and d (here in row eVIII). The smaller daughter cell c_{2v} originated from the unequal mitosis of c_2 during first differential mitosis is colored *green*. *engrailed* positive nuclei—*blue*, ectoteloblasts—*grey*, b_{1h} and d_{1h} as the first neuroblasts—*orange*. **d** Optical section of the horizontal plane of the left side of the caudal papilla received by confocal laser scanning microscopy. On either side of the proctodaeum (*pr*, here shown for the left side), a distinctive group of cells lies posterior to the mesoteloblasts. These cells (comprising about 20 cells) are arranged as spheres (indicated by the *white broken line*) and probably lead to the telson mesoderm. The arrangement of the telson ectoderm cells (*ec*) suggests that this putative telson mesoderm is formed by invagination of ectoderm cells from the posterior-most tip of the telson anlage

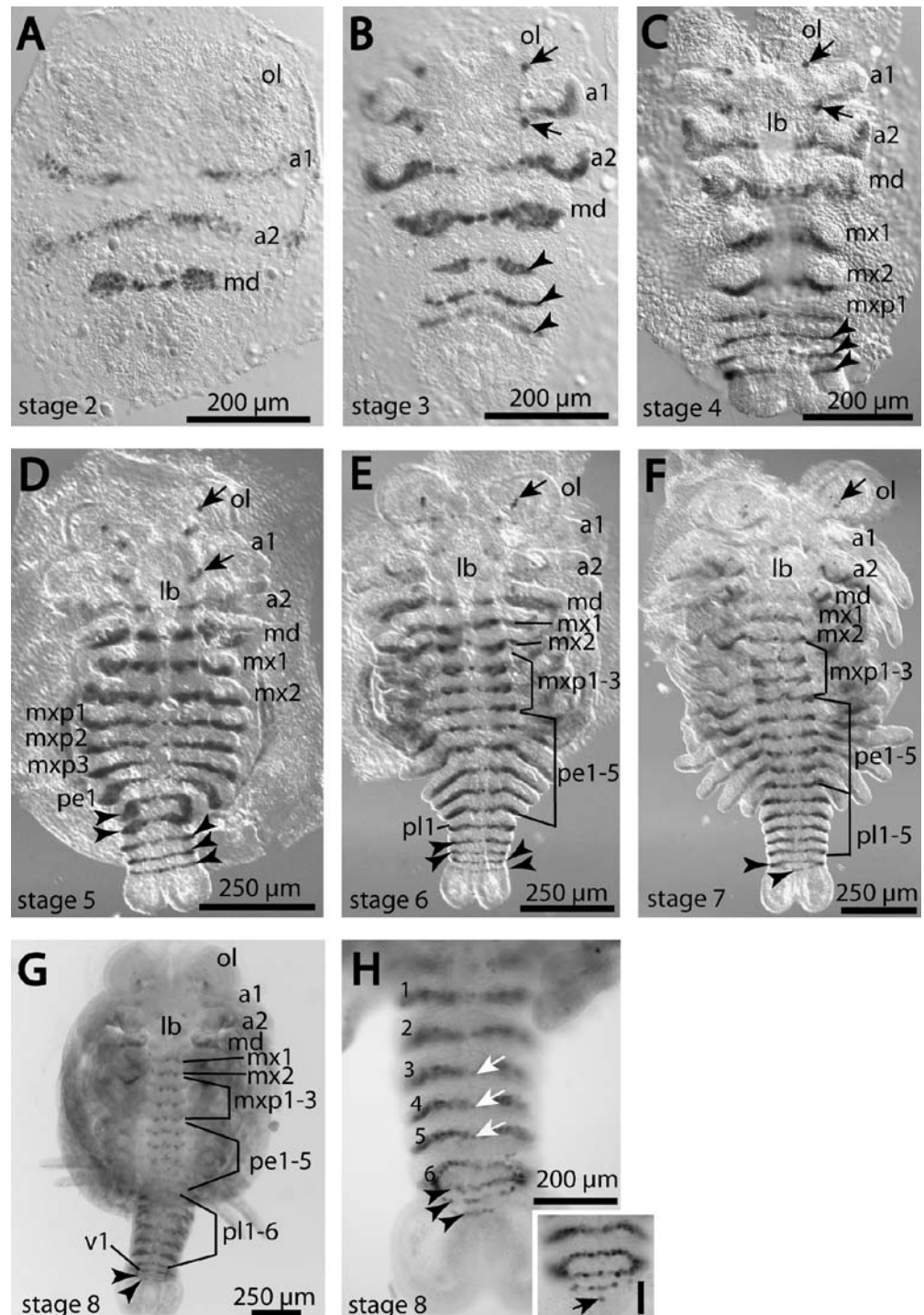
Cell lineage, *engrailed* expression and segment formation

Up to the formation of the post-naupliar segments, no specific cell division pattern is discernable (Fig. 2b–d). First, ectoteloblasts differentiate posterior to the naupliar segments, starting from the midline of the embryo and proceeding laterally during stage 3 (Fig. 2d,e). During the initial differentiation of the ectoteloblasts the ectoderm cells posterior to the mandibular segment are already

arranged in rows, indicating a non-ectoteloblastic origin of the cell material of the first maxillary segment (Fig. 2e). To what extent the segment of the second maxillae originates from ectoteloblast derivatives was not analyzed in the present study. However, posterior to the second maxillary segment, the ectoteloblasts already start proliferation of cells to the anterior, while the recruitment of ectoteloblasts more laterally is still in progress (Fig. 2f).

At the end of stage 3, ectoteloblast differentiation is completed and a ring of about 40 ectoteloblasts surrounds

Fig. 5 Expression pattern of *engrailed* in Marmorikrebs embryos from stage 2 to stage 8. **a** Embryo as the *V-shaped* germ band at the end of stage 2. Three *engrailed* positive stripes mark the posterior borders of the segments of the first and second antennae (*a1* and *a2*) and of the mandibles (*md*). *ol*—optical lobes. **b** Three additional *engrailed* positive stripes (arrowheads) occur during stage 4. Arrows designate the head spots. **c** Three additional *engrailed* positive stripes in an embryo at stage 5 (arrowheads). The posterior-most stripe marks the posterior border of the first pereiomere. *lb*—labrum, *mx1*—segment of the first maxillae, *mx2*—segment of the second maxillae, *mxp1*—segment of the first maxillipeds. **d** Five additional *engrailed* positive stripes (arrowheads). The posterior-most stripe is the posterior border of the first pleomere. *mxp2*—segment of the second maxillipeds, *mxp3*—segment of the third maxillipeds, *pe1*—first pereiomere. **e** Embryo at stage 6 with four additional *engrailed* stripes (arrowheads) compared to stage 5. *pe1–5*—first to 5th pereiomeres, *pl1*—first pleomere. **f** An embryo at stage 7 reveals the first *engrailed* stripe (*v1*) posterior to the pleonic stripes. **g** Overview of an embryo at stage 8 revealing the *engrailed* stripes of the complete set of segments and three additional stripes posterior to the 6th pleomere. **h** Detail of a caudal papilla during stage 8, anterior is up. Posterior to the six pleonic *engrailed* stripes, three additional stripes are expressed (arrowheads). White arrows in the segments 3 to 5 point to the median *engrailed* positive cells as the neuronal precursor cells. **i** Detail of the posterior-most part of the caudal papilla little earlier than in (**h**). The posterior-most stripe starts in one median cell (arrow)

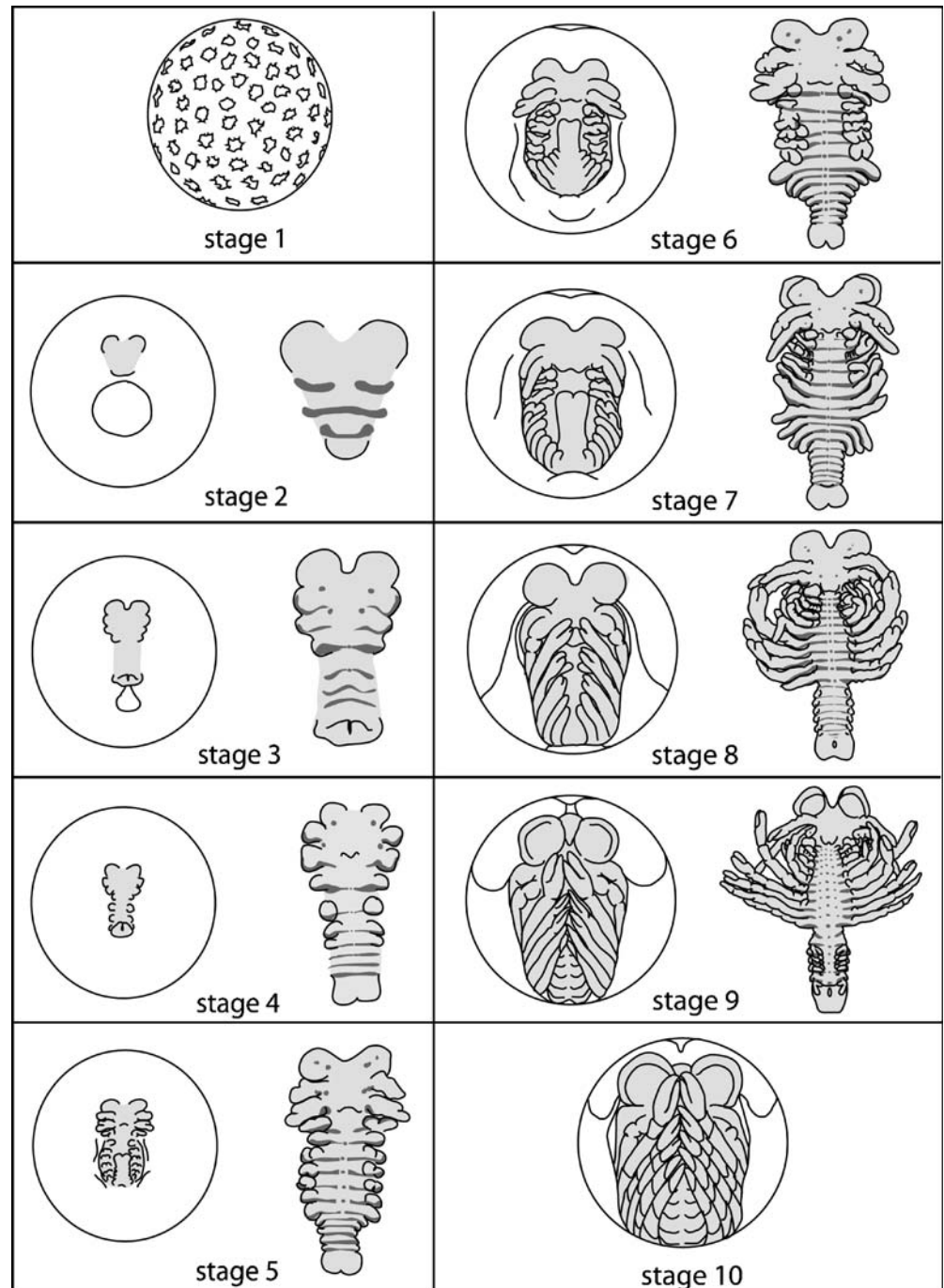


the posterior-most part of the embryo, the prospective caudal papilla (Figs. 2f and 4b). From now on, the ectoteloblasts proliferate the complete ectodermal cell material, from ventral to dorsal, of the following post-naupliar segments. They proliferate cells to the anterior that undergo two mediolateral mitotic waves and form the grid-like cell pattern consisting of the transverse descendant rows a, b, c, and d (Fig. 4b,c). A section comprising the descendant cells of a, b, c, and d forms one genealogical unit. These transverse cell rows then undergo the first differential mitotic wave (Fig. 4c). The first differential mitotic wave exhibits a stereotyped division pattern in

which each individual mitosis shows a characteristic spindle direction (Fig. 4c). For instance, in respect to the relative size of the daughter cells, the division of cell c_2 is clearly unequal, leading to the larger cell c_2h and smaller cell c_2v (Fig. 4c).

The segment polarity gene *engrailed* is expressed in the anterior descendants of each transverse ectoderm row (Fig. 4c). In the post-naupliar segments, the first expression of *engrailed* is detected after the first mediolateral mitotic wave in the transverse cell row ab (Fig. 4c). During the next mitotic wave, *engrailed* expression is lost in row b (Fig. 4c). The intersegmental furrows are formed posterior

Fig. 6 Schematic drawings of embryos in their position in the living eggs (at the *right-hand site* of each *box*) and schemes of embryos at stage 2 to 9 after fixation, with the caudal papilla folded back to have the view of the ventral ectoderm, and the carapace anlage removed (at the *left-hand site*). The region of the prospective ventral site of the embryo is shaded *light grey*. *Dark grey stripes/spots* in the embryos after preparation illustrate the *engrailed* stripes/secondary head spots



to the *engrailed* stripes, establishing the segmental borders (Fig. 4b). Thus, the transverse intersegmental furrows between the prospective segments form within the genealogical units and do not correspond to genealogical units.

The analysis of the *engrailed* expression pattern during development reveals that the onset of *engrailed* expression occurs during stage 2 and can be detected until the embryos have reached stage 9 (Figs. 5 and 6). An overview of *engrailed* stripe formation in relation to the morphological development at different stages is presented in Fig. 6. The posterior segmental borders of the naupliar segments of the first antennae, second antennae and mandibles first express *engrailed* in the V-shaped germ at the late stage 2 (Fig. 5a). These stripes appear more or less at the same time and it could not be decided in which segment *engrailed* expression is initiated. The segment of the first antennae reveals the expression in a stripe in each body half without a median connection. The stripes of the segment of the second antennae and the mandibles are continuous at this stage (Fig. 5a). The mandibular stripe forms one cell row in the median region and broadens laterally so that it appears barbell shaped (Fig. 5a).

During stage 3, three additional *engrailed* stripes occur posterior to the mandibular stripe, indicating the earliest anlage of post-naupliar segments at the level of gene expression (Fig. 5b). Like the following post-naupliar *engrailed* stripes, they appear in a strict antero-posterior direction, starting with the stripe of the first maxillary segment, followed by the stripe of the second maxillary segment and then by the stripe of the segment of the first maxilliped. At the segment border of the second antennal segment, the median cells lose the *engrailed* signal (Fig. 5b). Secondary head spots first occur during this stage in the ocular segment and in the segment of the first antennae (Fig. 5b). They remain detectable throughout the following development (see Fig. 5c–g).

During stage 4, the *engrailed* stripes of the three following segments, namely of the second and third maxillipeds and the first pereopods, are detectable. A diffuse *engrailed* signal appears in the carapace anlagen (Fig. 5c).

The stripes of the segments of pereopods 2 to 5 and of pleopods 1 are established at stage 5. In the region of the first and second antennae, the *engrailed* signal disappears except for the secondary headspots (Fig. 5d).

During stage 6, four additional stripes, the segmental borders of the pleomeres 2 to 5, are expressed (Fig. 5e). The *engrailed* stripe of the sixth pleomere occurs during stage 7. It is followed by the signal of an additional *engrailed* positive cell row posterior to the sixth pleomere during this stage (Fig. 5f). An embryo with the complete set of segments at stage 8 reveals the stripe of the mandibular segment, two stripes of the segments of the first and second maxillae, and eight stripes of the thoracic region (Fig. 5g). The pleonic region expresses, in addition to the six pleonic segments, three *engrailed* stripes in front of the telson (Fig. 5h,i).

Mesoteloblasts

The segmental mesoderm is proliferated by eight mesoteloblasts in the growth zone region of the caudal papilla forming an inner ring beneath the ectoteloblasts. Four mesoteloblasts (MT₁ to MT₄) are situated on either side of the proctodaeum. The MT₁s lie ventral to the proctodaeum directly beneath the ET₁ and the other three MTs in groups dorsolaterally to the proctodaeum. They proliferate the prospective mesoderm in the anterior direction with the mitotic phases slightly delayed compared to the mitotic waves of the ectoteloblasts (data not shown).

Telson

The region of the caudal papilla containing the opening of the proctodaeum posterior to the teloblasts gives rise to the telson. The amount of ectodermal cells of the telson is comparable to that of other crayfish and accordingly higher compared to that of other decapod embryos (see Scholtz 1993). The proctodaeum first opens dorsally near the tip of the caudal papilla. As the telson gets more and more differentiated, the opening of the proctodaeum becomes terminal at the early stage 6 and the proctodaeum then finally reaches the ventral side of the telson until stage 8. At stage 5, when the proctodaeum still opens dorsally, on either side of the opening a distinctive group of cells can be seen (Fig. 4d). These cell groups on each side (at stage 5 comprising about 20 cells) show a spherical arrangement (Fig. 4d). These cells probably form the telson mesoderm. The situation of the telson ectoderm cells in Fig. 4d suggests that this putative telson mesoderm is formed by an invagination of ectodermal cells from the tips of the telson bulbs.

Discussion

The parthenogenetic reproduction of the Marmorkrebs as the first occurrence within the decapod crustaceans represents a highly derived mode of reproduction. Studying embryonic aspects of the marbled crayfish implies the question to which extent these peculiarities are reflected in development. To address this question, Vogt et al. (2004) and Vogt and Tolley (2004) have investigated several aspects of the post-embryonic development. Seitz et al. (2005) have studied growth and reproduction parameters. In the present study, we focus on aspects of early development in more detail.

In general, the external morphological changes of the marbled crayfish correspond to those described in former studies of other bisexual freshwater crayfish (Reichenbach 1888; Zehnder 1934; Sandeman and Sandeman 1991; Celada et al. 1987, 1991). Some contradictions occur with respect to the staging of the Marmorkrebs by Seitz et al. (2005). According to these authors, the period of gastru-

lation extends for 29–39% of development. However, the 36% and 38% embryos shown in Seitz et al. (2005), (Figs. 7 and 8) correspond to our stage 4, i.e. the blastopore is already closed (Figs. 1e and 2g). Moreover, it appears to us that the 32% embryo (Seitz et al. 2005, Fig. 7) shows an earlier stage than the 29% embryo in the same figure. This conclusion is based on the fact that the initial blastopore is relatively large and decreases in size throughout development and that the dark area in front of the blastopore is the caudal papilla, which is more differentiated in the 29% stage than in the 32% stage of Seitz et al. (2005).

Our results reveal many correspondences to *Cherax destructor* (Sandeman and Sandeman 1991; Scholtz 1992). However, Sandeman and Sandeman (1991) describe the occurrence of the caudal papilla as a white crescent of cells combined with the closure of the blastopore as 15–20% development of *C. destructor*. The blastopore is closed in *C. destructor* at 20–25% development. In the marbled crayfish, the closure of the blastopore is slightly delayed with respect to the formation of the caudal papilla and the first appearance of the naupliar segment anlagen. The formation of the naupliar segment anlagen is already visible anterior to the caudal papilla as whitish patches, while the blastopore is still open. This is a clear case of heterochrony. However, it does not affect the correspondence in the external staging of *C. destructor* and the marbled crayfish.

The morphological development of limbs and other external structures is described based on SEM, such as with respect to the timing of limb bud splitting. Former studies on freshwater crayfish using SEM unfortunately did not go into enough detail to allow comparisons (Celada et al. 1987, 1991). For instance, the formation of paragnaths in the region of the mandibular sternite has not been described for crayfish, but it corresponds to the formation described in the peracarid *Orchestia cavimana* (Ungerer and Wolff 2005). Thus, this study might provide a basis for further studies on external development in freshwater crayfish as it is done for other malacostracans at the morphological and cellular levels (Dohle et al. 2004; Hejnol and Scholtz 2004; Ungerer and Wolff 2005).

Cell division pattern and *engrailed* gene expression

The cell lineage and the formation of the post-naupliar germ band of the Malacostraca is based on a complex and stereotyped cleavage pattern (Dohle and Scholtz 1988; Scholtz and Dohle 1996; Dohle et al. 2004). As in decapods in general, in the freshwater crayfish this ectodermal cell material is proliferated by ectoteloblasts surrounding the caudal papilla anterior to the telson (Scholtz 1993). The number of the ectoteloblasts in freshwater crayfish is about 40 and this is suggested to be an apomorphic character for the Astacida, derived from the character state of the ground pattern of the Malacostraca and other Decapoda which is suggested to be 19 ectoteloblasts (Scholtz 1993). The number of about 40 ectoteloblasts in the Marmorikrebs confirms this view.

With respect to our analysis of the cell division pattern of the post-naupliar germ band, we can show that the marbled crayfish corresponds in detail to *C. destructor* (Scholtz 1992; Scholtz et al. 1993). As shown for the first differential cleavage, not only are the individual spindles oriented in the same way but the relative size of the individual cells like c_{2v} and c_{2h} is also strikingly similar to that of *C. destructor* (Scholtz 1992).

The *engrailed* expression in the anterior descendants of each genealogical unit appearing in an anteroposterior direction is described for several malacostracans (e.g. Patel et al. 1989a; Scholtz et al. 1993; Abzhanov and Kaufman 2000b). The application of cross-reactive antibodies like *engrailed* to the marbled crayfish, as it is proposed in general for staging systems by Browne et al. (2005), provides an additional criterion to characterize fixed embryos. It is included in our staging system to enable an easy application in combination with other antibody-staining systems. Due to the easy and reliable antibody staining system of *engrailed* in the marbled crayfish, it could provide a basis for a finer resolution in combination with other antibody-staining systems, particularly if applied in a double staining system.

Our analysis of the cellular level of *engrailed* expression shows detailed similarities to what is found in other freshwater crayfish (Patel et al. 1989a; Scholtz et al. 1993): The initiation of *engrailed* expression during the first medio-lateral mitotic wave in row ab and the loss during the next mitosis in row b is found for the post-naupliar germ band in the Marmorikrebs. This phenomenon is not only described for *C. destructor* but is also known from *Neomysis integer* and other Malacostraca. In *Orchestia cavimana* and other amphipods, the *engrailed* expression is initialized later, namely, after the second mitotic wave in the transversal cell row a (Scholtz et al. 1993; Hejnol and Scholtz 2004; Browne et al. 2005).

The general *engrailed* expression pattern in the Marmorikrebs confirms the embryonic anlage of nine putative pleonic segments as is proposed for *C. destructor* (Scholtz 1995a) and as is also shown for *Procambarus clarkii* (Abzhanov and Kaufman 2000b).

All these results do not correspond to peculiarities that might be related to parthenogenesis during the development of the marbled crayfish. However, many questions, like e.g. the cell lineage of neurogenesis, still have to remain open and the marbled crayfish with its parthenogenetic reproduction mode might offer the chance to go into more detail due to the easy availability of a great amount of embryos independent from reproductive seasons.

Telson mesoderm

The formation of telson mesoderm is described for various malacostracans (Manton 1928, 1934; Shiino 1942; Weygoldt 1961). In the stomatopod *Squilla oratoria*, the telson mesoderm is formed by the immigration of peri-anal ectoderm cells starting with the elevation of the caudal

papilla up to the formation of the segment of the second maxilliped (Shiino 1942). Reviewing crustacean embryology, Shiino (1968) generally notes the origin of the telson mesoderm for crustaceans as an inward migration of ectodermal telson cells. In contrast, for the decapod *Palaemonetes varians*, Weygoldt (1961) describes the telson mesoderm as originating directly from the mesentoderm at the time of gastrulation. The telson mesoderm cells then start to proliferate after the caudal papilla has formed. They flank the proctodaeum as two groups of cells and, successively, these cell masses migrate in the anterior direction passing the region of the teloblasts (Weygoldt 1961). The formation of the telson mesoderm was not followed in the present study, but as shown in Fig. 4d, distinctive mesodermal cell groups indicate that the origin of the telson mesoderm might be based on the same process as described for *S. oratoria* (Shiino 1942).

Conjoined twins

Most morphological studies on decapod embryology exclude malformed embryos and only few descriptions of deviating morphogenesis can be found in earlier studies, such as the developmental study of the American lobster *Homarus americanus* by Herrick (1895). He also describes the occurrence of conjoined twins at different levels of development (Herrick 1895). More recently, Harzsch et al. (2000) analyzed the structure of the nervous system of a conjoined twin embryo (fused at the head region) of *H. americanus*. They discuss the impact of the partial fusion of the two embryo anlagen on the organization of the twin nervous systems (Harzsch et al. 2000). Another instance for the occurrence of a twin fused at the head region is described for the anomalan *Aegla abtao* (Jara and Palacios 2001).

The first report of conjoined twins in a freshwater crayfish was published for *Pacifastacus leniusculus* by Harlioğlu (2002). In this short note, the author interprets the anterior fusion in the head region up to the mandibular segment as an indication that the twin formation must have happened during naupliar segment formation (Harlioğlu 2002). In the case of the Marmorkrebs reported here, we think that the twin formation must have happened much earlier, at the latest during germ disc formation. All structures, including the growth zone, occur twice except for the lateral eye and the first antennal regions which are fused. In addition, the posterior margins of the carapace anlagen are conjoined. Accordingly, it is not a single embryo which underwent a split after the formation of the anterior naupliar segments, although at first sight it looks like that. What appears as one anterior head is in fact the right optic lobe and first antenna of the right embryo and the left optic lobe and first antenna of the left embryo. Interestingly, the anteroposterior axes of both embryos form a slight angle and it appears as if the two twins form one mirror axis between them. Whether or not the two embryos obey a mirror image symmetry of their handedness with respect to each other is not clear. The number of the fused segments is not fixed, as documentation of

conjoined twins in freshwater crayfish and lobsters reveal. Fusions can be observed not only in the head region, but also in the hind region (Herrick 1895, own unpublished data for *C. destructor*).

Until now, conjoined twins as well as malformed embryos are reported as unique events and more detailed studies of the impact on, for instance, the differentiation of teloblasts are missing for decapods in general. However, including these cases might contribute additional aspects to our understanding of developmental processes, and might provide a basis for further systematic research of the genetic control of crustacean development.

A staging system for crayfish development in general?

Freshwater crayfish are generally accepted as a well-supported monophyletic group. Some of the apomorphies apply to developmental characters, such as the invagination gastrula, the increased number ectoteloblasts of about 40, and the hatchling with the complete set of appendages except the first pleopods and uropods (Scholtz 1993, 1995b, 2002; Scholtz and Kawai 2002). It is also generally accepted that the freshwater crayfish comprise two monophyletic groups, the Parastacoidea of the Southern Hemisphere and the Astacoidea comprising all freshwater crayfish taxa of the Northern Hemisphere. Even if the phylogeny within these two groups is still controversially discussed (Scholtz 1995b, 2002; Crandall et al. 2000; Braband et al. 2006), the development of representatives of the different subtaxa of the Astacoidea (Reichenbach 1888; Celada et al. 1987, 1991) as well as of the Parastacoidea (Sandeman and Sandeman 1991; García-Guerrero et al. 2003) corresponds to each other in general, but even in respect to segment formation/differential cleavages (Scholtz 1992, this study). Thus, as argued by Sandeman and Sandeman (1991), a generalization on the developmental processes of freshwater crayfish seems to be reasonable.

Still, the description of continuous developmental processes always implies difficulties in the selection of the parameters on which certain developmental intervals can be discriminated to create a staging system. The most commonly used systems are based on either morphological events or on events scaled on time, often expressed in percentage of developmental time. These two staging types are discussed in detail by Bentley et al. (1979). Bentley et al. (1979) prefer the percentage system to the other systems for *Schistocerca nitens* for several reasons. According to the authors, the percentage method facilitates a more gradual determination and comparability between closely related taxa (Bentley et al. 1979). Taking into account that the Marmorkrebs, like other freshwater crayfish, varies in development within one clutch even at a constant temperature, the question is to what degree it is useful to characterize the developmental level of the marbled crayfish by less than 5% steps, as is done by Seitz et al. (2005). Even for *S. nitens*, in which the embryos of one pod develop very similar in time, the estimated error of the percentage staging is 1% (Bentley et al. 1979). In addition, we question the

advantage of the percentage method in respect to the comparability of developmental stages of different taxa with the same percentage assignment: first of all, the assignment of percentage varies even within the freshwater crayfish, showing that staging based on the percentage method does not inevitably mean that this method is more objective (see the deviations between the present study and Seitz et al. (2005) in the assignment of events). Secondly, the determination of percentages might also delude a precision in comparability even between closely related taxa. To avoid inconsistencies in the characterization of a developmental level, it might be more useful to reduce the number of developmental stages. In our opinion, a rough staging combined with morphological characters as shown above provides a more easily traceable basis for the first characterization and avoids misleading assignments.

The Marmorkrebs: a new model organism for Crustacea?

Due to its advantageous characteristics as a breeding animal and its high fecundity without great effort in laboratory equipment, the Marmorkrebs seems to have perfect requirements as a model organism. In this study it is shown for *engrailed*, but is also true for other gene products (unpublished data), that the marbled crayfish is very suitable for various techniques, such as antibody staining. Thus, it is an organism for studying freshwater crayfish development on different levels of developmental approaches as done for *P. clarkii* (Abzhanov and Kaufman 2000a,b) or at the level of genes as has been recently done for *C. destructor* (White et al. 2005).

As discussed above, it is reasonable to generalize developmental processes for the freshwater crayfish. The question arises in which respects it is useful to handle the development of the Marmorkrebs as a model organism representing developmental processes of the Crustacea in general. Thereby, it always has to be taken into account that the development of the Marmorkrebs, as of all other Astacida, represents a derived mode within the Crustacea in some aspects, such as the direct development combined with quite large and yolk-rich eggs undergoing superficial cleavage. Even within the decapods the freshwater crayfish represents a derived mode, for instance with respect to the increased number of ectoteloblasts etc. (see Scholtz 1993, 1995b). Above this, it should be considered that the phylogenetic position of the Astacida within the decapods is still unclear (e.g. Scholtz and Richter 1995; Schram 2001; Dixon et al 2003; Ah Yong and O'Meally 2004; Porter et al. 2005). Thus, it is necessary for comparative approaches to developmental processes to consider on which level processes are compared to those of other developmental systems and to test the extent to which homology hypotheses are possible. Development is, like adult structures, the subject to evolutionary change (Scholtz 2005).

Acknowledgements We are very grateful to Gabriele Drescher and to Wilfrid Bleiss, for the technical support using the SEM. We thank Greg Edgecombe for improving the English of the manuscript. We also thank Julia Pint for providing the photographs in Fig. 5h,i.

References

- Abzhanov A, Kaufman TC (2000a) Embryonic expression patterns of the Hox gene of the crayfish *Procambarus clarkii* (Crustacea, Decapoda). *Evol Dev* 2:271–283
- Abzhanov A, Kaufman TC (2000b) Evolution of distinct expression patterns for *engrailed* paralogs in higher crustaceans (Malacostraca). *Dev Genes Evol* 210:439–506
- Ahyong ST, O'Meally D (2004) Phylogeny of the Decapoda Reptantia: resolution using three molecular loci and morphology. *Raffles Bull Zool* 52:673–693
- Bentley D, Keshishian H, Shankland M, Toroian-Raymond A (1979) Quantitative staging of embryonic development of the grasshopper, *Schistocerca nitens*. *J Embryol Exp Morphol* 54:47–74
- Braband A, Kawai T, Scholtz G (2006) The phylogenetic position of the East Asian freshwater crayfish *Cambaroides* within the Northern Hemisphere Astacoidea (Crustacea, Decapoda, Astacida) based on molecular data. *J Zool Syst Evol Res* (in press)
- Browne WE, Price AL, Gerberding M, Patel NH (2005) Stages of embryonic development in the amphipod crustacean, *Parhyale hawaiiensis*. *Genesis* 42:124–149
- Celada JD, de Paz P, Gaudio VR, Fernández R (1987) Embryonic development of the freshwater crayfish (*Pacifastacus leniusculus* Dana): a scanning electron microscopic study. *Anat Rec* 219:304–310
- Celada JD, Carral JM, Gonzales J (1991) A study on the identification and chronology of the embryonic stages of the freshwater crayfish *Austropotamobius pallipes* (Lereboullet, 1858). *Crustaceana* 61:225–232
- Crandall KA, Harris DJ, Fetzner JW (2000) The monophyletic origin of freshwater crayfish estimated from nuclear and mitochondrial DNA sequences. *Proc R Soc Lond B* 267:1679–1686
- Dixon CJ, Ah Yong ST, Schram FR (2003) A new hypothesis of decapod phylogeny. *Crustaceana* 76:935–975
- Dohle W, Scholtz G (1988) Clonal analysis of the crustacean segment: the discordance between genealogical and segmental borders. *Development* 104(Suppl):147–160
- Dohle W, Gerberding M, Hejnol A, Scholtz G (2004) Cell lineage, segment differentiation, and gene expression in crustaceans. In: Scholtz G (ed) *Crustacean issues 15: evolutionary developmental biology of Crustacea*. Lisse, Balkema, pp 95–133
- Fioroni P (1969) Zum embryonalen und postembryonalen Dotteraufbau des Flusskrebsses (Astacus; Crustacea, Malacostraca, Decapoda). *Rev Suisse Zool* 47:919–946
- Fioroni P (1970) Am dotteraufschluß beteiligte Organe und Zelltypen bei höheren Krebsen; der Versuch zu einer einheitlichen Terminologie. *Zool Jb Anat* 87:481–522
- Fulinski B (1908) Beiträge zur embryonalen Entwicklung des Flußkrebsses. *Zool Anz* 33:20–28
- García-Guerrero M, Hendrickx ME, Villarreal H (2003) Description of the embryonic development of *Cherax quadricarinatus* (von Martens, 1868) (Decapoda, Parastacidae), based on the staging method. *Crustaceana* 76:269–280
- Gerberding M (1997) Germ band formation and early neurogenesis of *Leptodora kindti* (Cladocera): first evidence for neuroblasts in the entomostracan crustaceans. *Invertebr Reprod Dev* 32:63–73
- Harlioğlu MM (2002) The first report on the occurrence of twins in a freshwater crayfish, *Pacifastacus leniusculus* (Decapoda, Astacoidea). *Folia Biol (Krakow)* 50:215–216
- Harzsch S, Benton J, Beltz BS (2000) An unusual case of a mutant lobster embryo with double brain and double ventral nerve cord. *Arthropod Struct Dev* 29:95–99

- Hejnol A, Scholtz G (2004) Clonal analysis of distal-less and engrailed expression patterns during early morphogenesis of uniramous and biramous crustacean limbs. *Dev Genes Evol* 214:473–485
- Helluy SM, Beltz BS (1991) Embryonic development of the American Lobster (*Homarus americanus*): quantitative staging and characterization of an embryonic molt cycle. *Biol Bull* 180:355–371
- Herrick FH (1895) The American lobster: a study of its habits and development. *Bull US Fish Comm* 15:1–252(pl 54)
- Huxley TH (1880) The crayfish: an introduction in the study of zoology. C. Kegan Paul & Co., London
- Jara CG, Palacios VL (2001) Occurrence of conjoined twins in *Aegla abtao* Schmitt, 1942 (Decapoda, Anomura, Aegliidae). *Crustaceana* 74:1059–1065
- Lereboullet A (1862) Recherches d'embryologie comparée sur le développement du brochet, de la perche et de l'écrevisse. *Mém Acad Sci Inst Fr* 17:447–805
- Manton SM (1928) On the embryology of a mysid crustacean *Hemimysis lamornae*. *Philos Trans R Soc Lond B* 216:363–463
- Manton SM (1934) On the embryology of the crustacean *Nebalia bipes*. *Philos Trans R Soc Lond B* 498:163–238
- Olesen J, Richter S, Scholtz G (2003) On the ontogeny of *Leptodora kindtii* (Crustacea, Branchiopoda, Cladocera), with notes on the phylogeny of the Cladocera. *J Morphol* 256:235–259
- Patel NH, Kornberg TB, Goodman CS (1989a) Expression of engrailed during segmentation in grasshopper and crayfish. *Development* 107:201–212
- Patel NH, Martin-Blanco E, Coleman KG, Poole SJ, Ellis MC, Kornberg TB, Goodman CS (1989b) Expression of engrailed proteins in arthropods, annelids, and chordates. *Cell* 58:955–968
- Porter ML, Pérez-Losada M, Crandall KA (2005) Model-based multi-locus estimation of decapod phylogeny and divergence times. *Mol Phylogenet Evol* (in press)
- Rathke H (1829) Untersuchungen über die Bildung und Entwicklung des Flusskrebsses. Voss, Leipzig
- Reichenbach H (1888) Zur Embryonalentwicklung des Flußkrebsses. *Abh Senckenb Naturforsch Ges* 14:1–137
- Sandeman R, Sandeman D (1991) Stages in the development of the embryo of the fresh-water crayfish *Cherax destructor*. *Dev Biol* 200:27–37
- Sars GO (1873) Om en dimorph udvikling samt generationsvexel hos *Leptodora*. *Forh Videnskapsselsk Kristiania* 1–15
- Scholtz G (1992) Cell lineage studies in the crayfish *Cherax destructor* (Crustacea, Decapoda): germ band formation, segmentation, and early neurogenesis. *Roux's Arch Dev Biol* 202:36–48
- Scholtz G (1993) Teloblasts in decapod embryos: an embryonic character reveals the monophyletic origin of freshwater crayfishes (Crustacea, Decapoda). *Zool Anz* 230:45–54
- Scholtz G (1995a) Expression of the engrailed gene reveals nine putative segment-anlagen in the embryonic pleon of the freshwater crayfish *Cherax destructor* (Crustacea, Malacostraca, Decapoda). *Biol Bull* 188:157–165
- Scholtz G (1995b) Ursprung und Evolution der Flußkrebse (Crustacea, Astacida). *Sber Ges Naturf Freund Berlin* 34:93–115
- Scholtz G (1997) Cleavage, germ band formation and head segmentation: the ground pattern of the Euarthropoda. In: Fortey RA, Thomas RH (eds) *Arthropod relationships*. Chapman and Hall, London, pp 317–332
- Scholtz G (2002) Phylogeny and evolution. In: DM Holdich (ed) *Biology of freshwater crayfish*. Blackwell Science, Oxford, pp 30–52
- Scholtz G (2005) Homology and ontogeny: pattern and process in comparative developmental biology. *Theory Biosci* 124:121–143
- Scholtz G, Richter S (1995) Phylogenetic systematics of the reptantian Decapoda (Crustacea, Malacostraca). *Zool J Linn Soc* 113:289–328
- Scholtz G, Dohle W (1996) Cell lineage and cell fate in crustacean embryos—a comparative approach. *Int J Dev Biol* 40:211–220
- Scholtz G, Kawai T (2002) Aspects of embryonic and postembryonic development of the Japanese freshwater crayfish *Cambaroides japonicus* (Crustacea, Decapoda) including a hypothesis on the evolution of maternal care in the Astacida. *Acta Zool (Stockh.)* 83:203–212
- Scholtz G, Dohle W, Sandeman RE, Richter S (1993) Expression of engrailed can be lost and regained in cells of one clone in crustacean embryos. *Int J Dev Biol* 37:299–304
- Scholtz G, Braband A, Tolley L, Reimann A, Mittmann B, Lukhaup C, Steuerwald F, Vogt G (2003) Parthenogenesis in an outsider crayfish. *Nature* 421:806
- Schram FR (2001) Phylogeny of decapods: moving toward a consensus. *Hydrobiologia* 449:1–20
- Seitz R, Vilpoux K, Hopp U, Harzsch S, Maier G (2005) Ontogeny of the Marmorkrebs (marbled crayfish): a parthenogenetic crayfish with unknown origin and phylogenetic position. *J Exp Zool* 303A:393–405
- Shiino SM (1942) Studies on the embryology of *Squilla oratoria* de Haan. *Mem Coll Sci* 17:77–174
- Shiino SM (1968) I. Crustacea. In: Kumé M, Dan K (eds) *Invertebrate embryology*. Nolit, Belgrade, Yugoslavia 10, p 333–388
- Ungerer P, Wolff C (2005) External morphology of limb development in the amphipod *Orchestia cavimana* (Crustacea, Malacostraca, Peracarida). *Zoomorphology* 124:89–99
- Vogt G, Tolley L (2004) Brood care in freshwater crayfish and relationship with the offspring's sensory deficiencies. *J Morphol* 262:566–582
- Vogt G, Tolley L, Scholtz G (2004) Life stages and reproductive components of the Marmorkrebs (marbled crayfish), the first parthenogenetic decapod crustacean. *J Morphol* 261:286–311
- Weygoldt P (1961) Beitrag zur Kenntnis der Ontogenie der Dekapoden: Embryologische Untersuchungen an *Palaemonetes varians* (Leach). *Zool Jb Anat* 79:223–270
- White RB, Lamey TM, Ziman M, Koenders A (2005) Isolation and expression analysis of a Pax group III gene from the crustacean *Cherax destructor*. *Dev Genes Evol* 215:306–312
- Zehnder R (1934) Über die Embryonalentwicklung des Flusskrebsses. *Acta Zool* 15:261–408